

Hydrogen Bonding and Cation Coordination Effects in Primary and Secondary Amines Dissolved in Carbon Tetrachloride

Nathalie Rocher and Roger Frech*

Department of Chemistry and Biochemistry, University of Oklahoma, Norman, Oklahoma 73019

Received: September 18, 2006; In Final Form: February 1, 2007

Raman and infrared spectroscopy were used to investigate hydrogen-bonding interactions and cation coordination effects in solutions of lithium triflate (LiCF_3SO_3) dissolved in two primary amines, hexylamine (HEXA) and *N,N*-dimethylethylenediamine (DMEDA), and in a secondary amine, dipropylamine (DPA). Strong *intermolecular* hydrogen-bonding interactions and weaker *intramolecular* hydrogen-bonding interactions that occur only in DMEDA were spectroscopically distinguished in a comparison of pure HEXA, pure DMEDA, and the dilute solutions of these amines in CCl_4 . The spectroscopic shifts in intensity and frequency in the NH stretching region of DPA and DPA diluted in CCl_4 were similar to those of HEXA. Dilute electrolyte solutions in carbon tetrachloride were prepared to analyze specifically the cation coordination effect. In these solutions, limited intermolecular hydrogen-bonding interactions are present, and the observed spectral shifts correspond primarily to the cation-induced shifts. The symmetric SO_3 stretching region of the triflate anion was investigated to probe further the coordination of the cation. The local structures of the triflate ions and the amine groups in the electrolyte solutions dissolved in CCl_4 are similar to the local structures in the corresponding amine–salt crystals previously reported by us.

1. Introduction

Studies of the NH stretching vibrations in primary and secondary amines have been shown to be valuable in developing an understanding of the amino group hydrogen-bonding interactions. Most of the work has been conducted by analyzing the frequency shifts observed in the infrared spectra of amines and amines diluted in various nonpolar solvents, such as hexane, benzene, and carbon tetrachloride.^{1–5} The Raman intensities of the NH stretching vibrations are very weak compared to the infrared intensities, especially when the amine is diluted, and therefore have not been examined as thoroughly.

In the past few years, a variety of polymers containing amine groups have been examined for their potential application in lithium rechargeable batteries.^{6–13} Electrolytes are prepared from these materials by dissolving a salt into the polymer. Cation–host and cation–anion interactions play an important role in controlling the ionic conductivity of these materials. Vibrational spectroscopy has been widely used to study these interactions.^{14–17} However, in polymers that contain primary or secondary amine groups such as branched and linear poly(ethylenimine), the presence of ion-coordinating sites that also have the potential to participate in hydrogen-bonding interactions complicates the analysis of the spectra. Moreover, in amorphous polymeric materials, the large distribution of interactions is reflected in the breadth of the bands, which further complicates the spectra. The study of model compounds, i.e., small molecules whose structures mimic local structures found in the higher-molecular-weight systems, has been an efficient strategy to enhance our knowledge of the polymeric electrolytes.^{18–23} However, even in these small-molecular-weight electrolytes, the simultaneous presence of hydrogen-bonding interactions and the ion-coordinating effect complicates the analysis of NH stretching

vibrations. But by diluting these small molecules in nonpolar solvents, it is possible to minimize or eliminate intermolecular hydrogen-bonding interactions and analyze the frequencies of the “free” NH bands. Similarly, by diluting an electrolyte in a nonpolar solvent, it is possible to examine the effect of the salt on the small molecular host in the absence of intermolecular hydrogen-bonding interactions.

In this study, infrared and Raman spectroscopy are used to characterize the NH stretching vibrations of three model compounds and their complexes formed with lithium triflate, LiCF_3SO_3 (abbreviated LiTf). Hexylamine (HEXA) and *N,N*-dimethylethylenediamine (DMEDA) are primary amines, while dipropylamine (DPA) is a secondary amine. A comparative study of the infrared and Raman spectra of the pure amines combined with concentration-dependent measurements of their carbon tetrachloride solutions and amine–LiTf complexes in carbon tetrachloride solutions allowed an unambiguous separation of the effects of hydrogen-bonding interactions and lithium cation coordination.

2. Experimental

2.1. Sample Preparation. Hexylamine, *N,N*-dimethylethylenediamine, dipropylamine, and lithium trifluoromethane sulfonate, LiCF_3SO_3 (LiTf), were obtained from Aldrich. All the amines were used as received. The LiTf was dried under vacuum at 120 °C for 48 h before use. Carbon tetrachloride was obtained from Fischer Scientific (99.9%, A.C.S. reagent) and distilled before use. The chemicals were stored and used in a dry argon atmosphere glove box ($\text{VAC} \leq 1 \text{ ppm H}_2\text{O}$) at room temperature. The amine–LiTf complexes were prepared by mixing weighed amounts of amines and LiTf; the solutions were stirred for a minimum of 24 h before use. The compositions of the samples are reported as the nitrogen to cation molar ratio (N/Li^+). The amine– CCl_4 solutions were prepared by mixing weighed amounts of amines and CCl_4 . The compositions of these

* Corresponding author. Email: rfrech@ou.edu. Telephone: 405-325-3831. Fax: 405-325-6111.

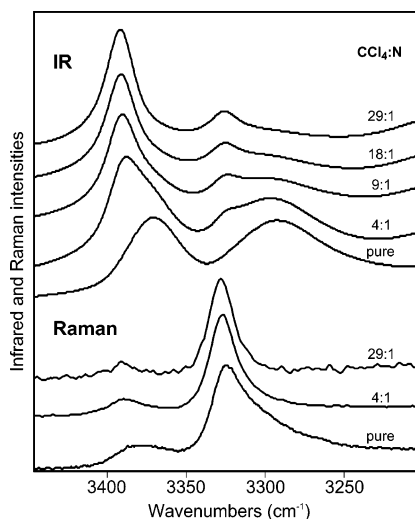


Figure 1. Infrared (top) and Raman (bottom) spectra of the N–H stretching region for pure HEXA and HEXA dissolved in carbon tetrachloride at different concentrations (reported as CCl₄/N molar ratios).

samples are reported as a CCl₄ to nitrogen molar ratio (CCl₄/N). Similarly, the amine–LiTf solutions in CCl₄ were prepared by mixing weighed amounts of the components. The compositions of these samples are also reported as a CCl₄ to nitrogen molar ratio.

2.2. FT–IR and Raman Spectroscopy. All of the infrared samples were recorded using a sealed liquid cell equipped with potassium bromide windows. Infrared data were collected using a Bruker IFS66V FT–IR spectrometer (KBr beam splitter) under dry air purge. The data were recorded over a range of 500–4000 cm^{−1} with a spectral resolution of 1 cm^{−1}. The FT–Raman samples were sealed in a thin NMR tube under an argon atmosphere. The data were recorded at 2 cm^{−1} resolution using a Bruker Equinox 55 equipped with a FRA 106/S system. The 1064 nm line of a Nd:YAG laser was used for excitation. Curve-fitting analysis of the N–H stretching bands was done using commercially available software (Thermo Galactic, Grams/AI 7.00). The spectral bands were fitted using mixed Gaussian/Lorentzian product functions and a straight baseline.

3. Results and Discussion

3.1. Hexylamine: A Simple Primary Amine. The infrared and Raman spectra of HEXA in the NH stretching region contain the antisymmetric stretch, $\nu_{as}(\text{NH}_2)$, the symmetric stretch, $\nu_s(\text{NH}_2)$, and the first overtone of the NH₂ deformation band (superposed in the two spectra and lower in frequency). In the infrared spectrum, $\nu_{as}(\text{NH}_2)$ and $\nu_s(\text{NH}_2)$ have about the same intensity and occur at 3371 and 3293 cm^{−1}, respectively. In the Raman spectrum, the scattering intensity of $\nu_s(\text{NH}_2)$ at 3324 cm^{−1} is large compared to that of $\nu_{as}(\text{NH}_2)$ at 3376 cm^{−1} (Figure 1).

A careful comparison of the two spectra taking into account the selection rules for IR and Raman has allowed a deeper understanding of hydrogen-bonding interactions in HEXA.²⁴ The long tail on the low-frequency side of the $\nu_s(\text{NH}_2)$ in the Raman spectrum indicates the presence of molecules that are more strongly hydrogen bonded than the molecules contributing to the intensity in the vicinity of the band maximum. This lower-frequency tail corresponds with the maximum IR intensity of this mode. By contrast, the intensity and frequency of the $\nu_{as}(\text{NH}_2)$ mode are less sensitive to hydrogen-bonding interac-

tions than the $\nu_s(\text{NH}_2)$ mode, as seen by the small differences in the frequencies between the IR and Raman spectra.

When HEXA is diluted in carbon tetrachloride, the interactions between the HEXA molecules decrease to a significant degree. In very dilute solutions, the vibrations of the NH₂ group are expected to behave as “free” molecules. Figure 1 shows a superposition of the IR and Raman spectra of pure HEXA and various compositions of HEXA dissolved in CCl₄. In the Raman spectra, the $\nu_{as}(\text{NH}_2)$ band shifts from 3376 cm^{−1} (pure HEXA) to about 3390 cm^{−1} in the most dilute solution (29:1 CCl₄/HEXA molar ratio). The maximum intensity of the $\nu_s(\text{NH}_2)$ band shifts slightly from 3324 cm^{−1} (pure HEXA) to 3328 cm^{−1} in the most dilute solution. The intensity of the low-frequency tail in pure HEXA decreases in the 4:1 solution. Upon further dilution (18:1 solution), the intensity of the tail further decreases so that the shape of the $\nu_s(\text{NH}_2)$ band is symmetrical and centered at 3328 cm^{−1}. There are no additional spectral changes at higher dilutions. The Raman frequency of the $\nu_s(\text{NH}_2)$ band of pure HEXA is only 4 cm^{−1} lower than that in the dilute solutions. This is expected because the Raman scattering intensity is larger for symmetric modes. Therefore, the Raman spectrum of pure HEXA selectively samples molecules that are undergoing minimal or no hydrogen-bonding interactions, and very little spectral change should occur upon dilution.²⁴

The concentration dependence of HEXA in CCl₄ is also shown in the infrared spectrum in Figure 1. In pure HEXA, the broad $\nu_s(\text{NH}_2)$ band occurs at 3293 cm^{−1}; upon dilution, a shoulder appears around 3324 cm^{−1} on the high-frequency side of the band. As the solution becomes more dilute, the shoulder grows in intensity and the original band progressively decreases. When the composition reaches 29:1, the original band at 3293 cm^{−1} has mostly disappeared and is replaced by a new band at 3326 cm^{−1}.

In contrast to the symmetric stretch, the $\nu_{as}(\text{NH}_2)$ band seems to shift progressively to higher frequencies, but in fact, its behavior is very similar to that of the symmetric stretch. At a 4:1 composition, the maximum intensity of the band is at 3388 cm^{−1} with a shoulder on the low-frequency side. Upon further dilution, the maximum intensity of the band slightly shifts to 3392 cm^{−1} in the 29:1 sample, and the shoulder disappears. A curve fitting analysis of the 9:1 composition spectrum shows that the antisymmetric stretch is composed of two peaks at 3391 and 3369 cm^{−1}, and the symmetric stretch contains two peaks at 3325 and 3299 cm^{−1}. For both the antisymmetric and the symmetric stretches, the high-frequency band corresponds to a population of HEXA molecules that are mostly “free”. The frequencies of these bands are similar in the IR and in the Raman spectra within ± 2 wavenumbers. The lower-frequency bands observed in the IR spectra correspond to HEXA molecules that undergo relatively strong hydrogen-bonding interactions.

It is important to note the relative intensity changes of the two NH stretches in the IR spectra as HEXA is diluted with CCl₄. In pure HEXA, the IR intensities of $\nu_{as}(\text{NH}_2)$ and $\nu_s(\text{NH}_2)$ are roughly equivalent. In dilute solutions, hydrogen-bonding interactions are greatly reduced; as a result, the two hydrogen atoms of the amine group have approximately equivalent potential energy environments, and the symmetric and antisymmetric nature of the vibrational modes is easily observed. In the most dilute solution, the intensity of $\nu_{as}(\text{NH}_2)$ is markedly greater than that of $\nu_s(\text{NH}_2)$. By contrast, the Raman intensity of $\nu_s(\text{NH}_2)$ is greater than $\nu_{as}(\text{NH}_2)$ in all solutions and pure HEXA because the Raman measurement selects those molecules with the least amount of hydrogen-bonding interactions as noted earlier.

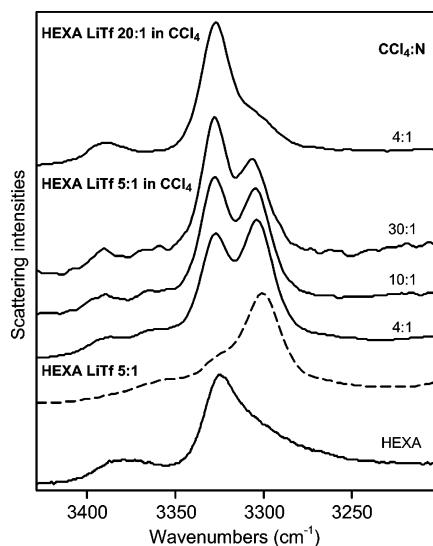


Figure 2. Raman spectra of HEXA–LiTf 5:1 (N/Li molar ratio) superposed with the Raman spectra of HEXA–LiTf 5:1 and HEXA–LiTf 20:1 diluted in CCl₄ at different concentrations (reported as CCl₄/N molar ratios) in the N–H stretching region.

When a salt is dissolved in a primary amine, there are two effects that change the vibrational modes, particularly the N–H stretching vibrations: the breaking of the hydrogen bonds and the cation effect as it coordinates the nitrogen atom. The lithium ion is coordinated to the NH₂ group through the lone pair of the nitrogen atom, which changes the electronic distribution in the NH₂ group. This interaction weakens the N–H bond by decreasing its electron density and thereby decreases the mode frequency. There is an additional competing effect if the anions can undergo hydrogen-bonding interactions with the nitrogen atoms. In that case, coordination of the nitrogen by the cation can reduce hydrogen bonding, thus increasing the mode frequency. We have previously attempted to sort these two effects in a several studies.^{13,24}

Diluting HEXA molecules in a CCl₄ solution allows a study of the primary amine vibrational group when very limited intermolecular hydrogen bonding is present. Therefore, adding an electrolyte to a dilute solution of HEXA in CCl₄ allows one to study the effect of salt addition on the molecular host in the absence of significant intermolecular hydrogen-bonding interactions.

Two solutions of different concentrations of HEXA–LiTf electrolyte were dissolved in CCl₄. The results are very illuminating. Figure 2 shows the Raman spectra of HEXA–LiTf 5:1 (N/Li molar ratio) superposed with the Raman spectra of HEXA–LiTf 5:1 diluted in CCl₄ at different concentrations (reported as CCl₄/N molar ratios).

The antisymmetric stretch has a very weak Raman scattering intensity; therefore only limited information can be obtained from this mode. The symmetric stretch of the HEXA–LiTf 5:1 solution occurs at 3300 cm⁻¹ with a shoulder around 3325 cm⁻¹. The $\nu_s(\text{NH}_2)$ region of all HEXA–LiTf 5:1 complexes dissolved in CCl₄ clearly contain two bands; in the most dilute solution (CCl₄/N = 30:1), these occur at 3328 and 3306 cm⁻¹. The scattering intensity of the former mode increases with increasing dilution and originates from HEXA molecules not undergoing hydrogen-bonding interactions or a cation-induced shift, as noted in the previous discussion. The band at 3306 cm⁻¹ originates in HEXA molecules undergoing a cation-induced shift (cation coordination effect) but no hydrogen-bonding interactions. Because the nitrogen to lithium ratio is fixed at 5:1, the

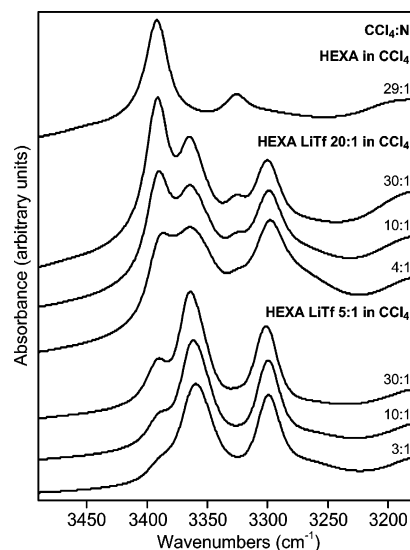


Figure 3. Infrared spectra of HEXA diluted in CCl₄ at a 29:1 composition superposed with HEXA–LiTf 20:1 and HEXA–LiTf 5:1 diluted in CCl₄ at different concentrations (reported as CCl₄/N molar ratios) in the N–H stretching region.

population of HEXA molecules undergoing the lithium ion coordination effect is constant. Therefore the intensity increase of the higher-frequency mode with dilution reflects the growing population of “free” HEXA molecules that have significant Raman activity. *The strength of the cation–nitrogen coordinative interaction can be measured by the 22 cm⁻¹ shift to lower frequencies.*

In the Raman spectrum of HEXA–LiTf 20:1 in CCl₄ at a 4:1 CCl₄/N ratio (also shown in Figure 2), the population of HEXA molecules experiencing the coordination effect is very small because of the relatively few lithium cations present. The cation-shifted band is only seen as a shoulder on the low-frequency side of the 3328 cm⁻¹ band.

The infrared spectra of a series of HEXA–LiTf 5:1 and HEXA–LiTf 20:1 compositions diluted in CCl₄ at various concentrations (reported as CCl₄/N molar ratios) are shown in Figure 3. In both LiTf compositions, the $\nu_{as}(\text{NH}_2)$ region has two bands at 3391 and 3365 cm⁻¹ in the most dilute solutions, with the intensity of the higher-frequency mode increasing with dilution relative to the lower-frequency mode. In the $\nu_s(\text{NH}_2)$ region of HEXA–LiTf 20:1, one main band occurs at 3300 cm⁻¹ and a weak band starts to grow upon dilution, reaching 3326 cm⁻¹ in the most dilute solution. In contrast, in HEXA–LiTf 5:1, only one band is observed at 3301 cm⁻¹. The NH₂ vibrations at 3391 and 3326 cm⁻¹ from the $\nu_{as}(\text{NH}_2)$ and the $\nu_s(\text{NH}_2)$ modes, respectively, have been attributed to the “free” NH₂ groups. This assignment is supported by the IR and Raman spectra of the most dilute HEXA–CCl₄ solution because the frequencies of the two NH₂ stretching modes correspond within ± 2 cm⁻¹, as shown in Figure 3. In both the antisymmetric and symmetric stretching regions, the increase in intensity of the higher-frequency mode with dilution reflects an increase in the population of “free” HEXA molecules relative to the hydrogen-bonded molecules. This increase was previously noted in the Raman and IR spectra of HEXA diluted in CCl₄ and in the Raman spectra of HEXA–LiTf 5:1 in CCl₄. The lower-frequency bands of $\nu_{as}(\text{NH}_2)$ and $\nu_s(\text{NH}_2)$ (3365 and 3301 cm⁻¹ in the most dilute solutions) are assigned to HEXA molecules coordinated by lithium with weak intermolecular hydrogen-bonding interactions between HEXA molecules. These hydrogen-bonding interactions decrease with dilution until, in the most

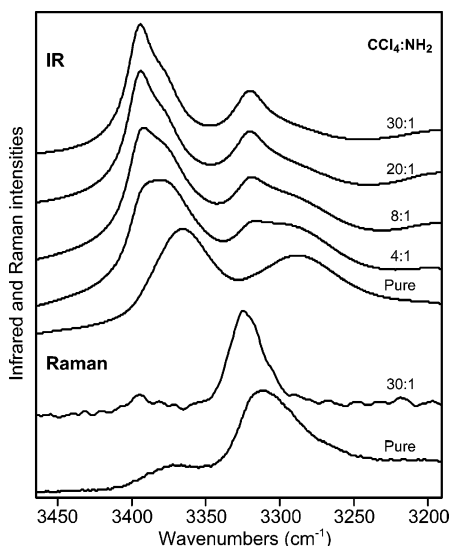


Figure 4. Infrared (top) and Raman (bottom) spectra of the N–H stretching region for pure DMEDA and DMEDA dissolved in carbon tetrachloride at different concentrations (reported as CCl_4/NH_2 molar ratios).

dilute solutions, intermolecular hydrogen bonding is essentially eliminated and the frequencies of these bands are due almost entirely to the cation coordination effect.

For a given nitrogen to lithium ratio, the number of HEXA molecules undergoing a coordination effect appears to be independent of the degree of dilution in CCl_4 . When the amount of salt in the system increases (i.e., from a 20:1 to a 5:1 N/Li ratio), the population of molecules that are coordinated with lithium increases, as reflected by the relative intensities of the two $\nu_{\text{as}}(\text{NH}_2)$ modes in the two different dilution series. At a 5:1 N/Li ratio, the intensity of the 3365 cm^{-1} band, which is due to lithium-coordinated HEXA molecules, is very large compare to the “free” NH_2 band at 3391 cm^{-1} . In contrast, in the 20:1 N:Li solution, the bands at 3391 and 3365 cm^{-1} have similar intensities, indicating a substantial amount of HEXA molecules not affected by the salt. This argument is also supported by the $\nu_{\text{s}}(\text{NH}_2)$ region, where the presence of a “free” HEXA population is observed only in the HEXA–LiTf 20:1 dilution series.

The bands that are shifted to lower frequencies around 3365 and 3301 cm^{-1} have been assigned to the population of amine groups that are coordinated with lithium. These frequencies differ from those of the IR of HEXA–LiTf (not diluted), where a mixture of hydrogen-bonding interactions and the coordination effect alter the vibrational frequencies of the modes. On the other hand, the frequency of the $\nu_{\text{s}}(\text{NH}_2)$ band at 3301 cm^{-1} corresponds to that of the Raman spectrum of HEXA–LiTf (not diluted), where it was shown that the measurement samples the molecules that are the least hydrogen bonded and therefore more directly show the coordinative effect of lithium.

To further the investigation of the amine–LiTf complexes dissolved in CCl_4 , spectral regions containing bands sensitive to ionic association are examined. The symmetric SO_3 stretch^{17,25,26} and the symmetric CF_3 deformation^{26–28} bands of the triflate molecule are particularly sensitive to cation–anion interactions in an electrolyte. The vibrational frequencies of these modes increase as the triflate anion becomes more highly associated. Unfortunately, CCl_4 bands interfere with the CF_3 deformation region in the IR and Raman spectra. The SO_3 stretching region is free of CCl_4 modes, but in the IR spectra, this region contains HEXA, DMEDA, or DPA modes. The

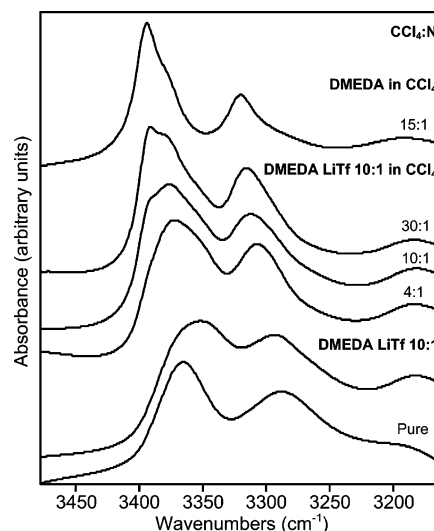


Figure 5. Infrared spectra of DMEDA–LiTf 10:1 (N/Li molar ratio) superposed with the infrared spectra of DMEDA diluted in CCl_4 at a 15:1 composition and DMEDA–LiTf 10:1 diluted in CCl_4 at different concentrations (reported as CCl_4/N molar ratios) in the N–H stretching region.

investigation of ionic association via the triflate bands is therefore limited to the $\nu_{\text{s}}(\text{SO}_3)$ region of the Raman spectra.

In the Raman spectra of HEXA–LiTf 5:1 in CCl_4 , the $\nu_{\text{s}}(\text{SO}_3)$ band shifts from 1046 to 1050 cm^{-1} with a shoulder around 1060 cm^{-1} upon dilution, indicating either a strengthening of the lithium–triflate interaction or an increase of the degree of ionic association. This trend can be correlated with the NH stretching region, where the $\nu_{\text{s}}(\text{NH}_2)$ band originating from the HEXA molecules interacting with the lithium slightly shifts from 3304 cm^{-1} in the 3:1 solution to 3306 cm^{-1} in the 30:1 solution, indicating that the strength of the lithium–nitrogen interaction slightly decreases upon dilution. In other words, the increase in ionic association is accompanied by a decrease in the lithium– NH_2 interaction. It is noteworthy that, as the solution becomes more dilute, the frequency of the $\nu_{\text{s}}(\text{SO}_3)$ band approaches 1053 cm^{-1} , the frequency of $\nu_{\text{s}}(\text{SO}_3)$ observed in a crystal of HEXA–LiTf.²⁴ As the effects of intermolecular hydrogen bonding are reduced with dilution, the lithium–triflate–HEXA interactions become more similar (on a very local scale) to those interactions in the crystalline phase.

3.2. *N,N*-Dimethylethylenediamine: A More Complex Primary Amine Molecule. The vibrations of the primary amine group in DMEDA are similar in some ways to those of HEXA. However, the presence of a tertiary amine nitrogen separated from the primary amine group by an ethylene structure leads to the possibility that one of the NH_2 hydrogen forms an intramolecular hydrogen bond. Gas-phase quantum chemical calculations of pure DMEDA show that the conformation favorable for intramolecular hydrogen bonding is energetically stable.²⁹ The possibility of intramolecular hydrogen-bonding complicates the vibrational analysis of the primary amine group. In spite of this, the general picture developed in the HEXA study is still valid.

Infrared and Raman spectra of DMEDA diluted in carbon tetrachloride resemble those of HEXA. However, there are noticeable differences that point toward different types of hydrogen-bonding interactions occurring in DMEDA. In the IR spectrum of the pure compound, $\nu_{\text{as}}(\text{NH}_2)$ and $\nu_{\text{s}}(\text{NH}_2)$ occur at 3366 and 3288 cm^{-1} , respectively. When DMEDA is

TABLE 1: IR Frequencies for the $\nu_{as}(\text{NH}_2)$ and the $\nu_s(\text{NH}_2)$ Modes of DMEDA Diluted in CCl_4^a

CCl_4/N	$\nu_{as}(\text{NH}_2)$		$\nu_s(\text{NH}_2)$	
	“free”	H-bonded	“free”	H-bonded
15:1	3395	3379	3320	3295

^a The 15:1 CCl_4/N molar ratio is equivalent to a 30:1 CCl_4/NH_2 molar ratio.

dissolved in CCl_4 (Figure 4), the $\nu_{as}(\text{NH}_2)$ and $\nu_s(\text{NH}_2)$ bands shift to higher frequencies, as was seen in CCl_4 solutions of HEXA.

However in the DMEDA– CCl_4 solutions, both bands also exhibit low-frequency shoulders. At a 30:1 CCl_4/NH_2 molar ratio (or 15:1 CCl_4/N molar ratio), band deconvolution shows that $\nu_{as}(\text{NH}_2)$ has bands at 3395 and 3379 cm^{-1} , while $\nu_s(\text{NH}_2)$ has bands at 3320 and 3295 cm^{-1} . The presence of two distinct bands for each of the symmetric and antisymmetric modes can be interpreted as originating in two different potential energy environments of the DMEDA molecules. In the more dilute solution, $\nu_{as}(\text{NH}_2)$ at 3395 cm^{-1} and $\nu_s(\text{NH}_2)$ at 3320 cm^{-1} result from the “free” amine groups and the $\nu_{as}(\text{NH}_2)$ at 3379 cm^{-1} and $\nu_s(\text{NH}_2)$ at 3295 cm^{-1} result from amine groups in a more hydrogen-bonded environment: possibly *intramolecularly* hydrogen-bonded molecules. This type of hydrogen bond is weaker in DMEDA than intermolecular hydrogen bonds because the H···N bond distance is limited by the conformation of the N–C–C–N backbone. Consequently, the frequencies corresponding to intramolecular hydrogen-bonded molecules are higher than in pure DMEDA, where a combination of inter- and intramolecular hydrogen bonds are present.

The Raman spectrum of pure DMEDA is also shown in Figure 4 along with the spectrum of the most dilute solution. In the pure molecule, the band maximum of $\nu_s(\text{NH}_2)$ at 3311 cm^{-1} is lower than that in HEXA, reflecting a more strongly hydrogen-bonded environment. A tail on the low-frequency side of the band is attributed to a distribution of populations that are more strongly hydrogen bonded than the molecules, contributing to the intensity in the band center. In the 30:1 CCl_4 solution, the band shifts to 3324 cm^{-1} and the intensity of the low-frequency wing decreases to leave a more symmetrical band. In the Raman spectrum, there is no clear evidence of two different types of populations. Strong Raman intensities result primarily from symmetrical vibrational modes. The presence of intramolecular hydrogen-bonding interactions alters the symmetric nature of the mode, and the Raman intensity decreases in consequence.

When salt is added to DMEDA, the changes observed in the Raman spectrum are not as dramatic as in the HEXA system and do not provide significant new information. In brief, DMEDA–LiTf 10:1 and DMEDA–LiTf 4:1 compositions were dissolved in various amounts of CCl_4 (spectra not shown). The $\nu_s(\text{NH}_2)$ band shifts to 3322 cm^{-1} in all the dilute solutions, and the intensity of the low-frequency wing progressively decreases as the DMEDA–LiTf complex becomes more diluted in CCl_4 , but the wing never completely disappears. Unlike the HEXA–LiTf system, no large shift to lower frequency is observed. This behavior is in accordance with the Raman spectra measured for the concentration dependence of DMEDA–LiTf with no addition of CCl_4 . It appears that a rough balance between the breaking of hydrogen bonds and the coordination effect of lithium prevents any large frequency shifts from occurring.³⁰ The small changes in the Raman spectra of the dilute solutions do not permit a detailed analysis. The different spectral behavior in the HEXA and DMEDA systems may be

TABLE 2: IR Frequencies for the $\nu_{as}(\text{NH}_2)$ and the $\nu_s(\text{NH}_2)$ Modes of DMEDA–LiTf 10:1 Diluted in CCl_4^a

CCl_4/N	$\nu_{as}(\text{NH}_2)$			$\nu_s(\text{NH}_2)$		
	“free”	H-bonded	complex	“free”	H-bonded	complex
30:1	3394	3380	3363	3319	3285	3306
10:1	3395	3381	3364	3319	3289	3306
4:1	not converged			not converged		

^a The ratios are CCl_4/N molar ratios.

due to differences in the cation coordination strength, as well as differences in the types of hydrogen bonds present. In DMEDA, lithium coordinates two nitrogens from the same molecule, whereas in HEXA, only one nitrogen atom is available. In both electrolyte solutions, the coordination of lithium is satisfied via the triflate anion oxygen atoms.

In contrast to the Raman spectra, the IR spectra of DMEDA–LiTf 10:1 dissolved in CCl_4 shows marked changes upon dilution. The data are shown in Figure 5, along with the IR spectrum of DMEDA diluted in CCl_4 at a 15:1 molar ratio.

Curve fitting of the three different CCl_4 dilutions of 10:1 DMEDA–LiTf shows that the original bands found in diluted DMEDA are still present when salt is added. A summary of the band deconvolution results is given in Tables 1 and 2 as an aid for the following discussion.

The two bands present in the DMEDA– CCl_4 solutions for each of the symmetric and antisymmetric stretches are also present in the DMEDA–LiTf– CCl_4 solutions, which indicate that the added salt does not affect the entire DMEDA population. As the concentration of DMEDA–LiTf complex increases, the intensities of the “free” and hydrogen-bonded DMEDA bands decrease and the intensities of the bands that correspond to the DMEDA–LiTf complex increase. For the 30:1 and 10:1 dilutions in CCl_4 , the curve fitting analysis resulted in converged solutions from which several conclusions may be drawn. The DMEDA–LiTf complex in CCl_4 has a symmetric NH_2 stretching vibration around 3306 cm^{-1} and an antisymmetric stretching vibration around 3364 cm^{-1} . As the concentration of the DMEDA–LiTf complex increases to a 4:1 composition (CCl_4/N molar ratio), the appearance and frequencies of the $\nu_s(\text{NH}_2)$ and $\nu_{as}(\text{NH}_2)$ become more similar to that of the undiluted complex, where a greater degree of inhomogeneity is reflected by the breadth of the bands. At this solution composition, the population of free primary amine groups is small and the sample is mainly composed of hydrogen-bonded amines and amines coordinated with lithium ions. The curve fitting analysis did not converge, apparently because of the large number of broad, overlapping bands in this region.

The N–H stretching frequencies of the DMEDA–LiTf complex in CCl_4 (Table 2) are very close to those of HEXA–LiTf in CCl_4 . The frequency of the $\nu_{as}(\text{NH}_2)$ vibration occurs around 3364 cm^{-1} for both complexes in CCl_4 . In contrast, the frequency of the $\nu_s(\text{NH}_2)$ vibration is about 5 cm^{-1} higher in the DMEDA complex (3306 vs 3301 cm^{-1} in HEXA–LiTf 5:1 in CCl_4 30:1). This 5 cm^{-1} difference is due to the higher sensitivity of the symmetric NH_2 stretching mode to the hydrogen-bonding environment of the amine group compared to the antisymmetric stretching mode. This also explains the difference between the $\nu_s(\text{NH}_2)$ frequency of the hydrogen-bonded population in the DMEDA–LiTf in CCl_4 (3285–3289 cm^{-1}) and DMEDA in CCl_4 (3295 cm^{-1}).

In the most concentrated DMEDA– CCl_4 solution, the triflate ion $\nu_s(\text{SO}_3)$ band occurs at 1040 cm^{-1} and has a shoulder around 1033 cm^{-1} . Upon increasing dilution, the band shifts to 1042 cm^{-1} and the shoulder disappears. In the 3:1 DMEDA–LiTf

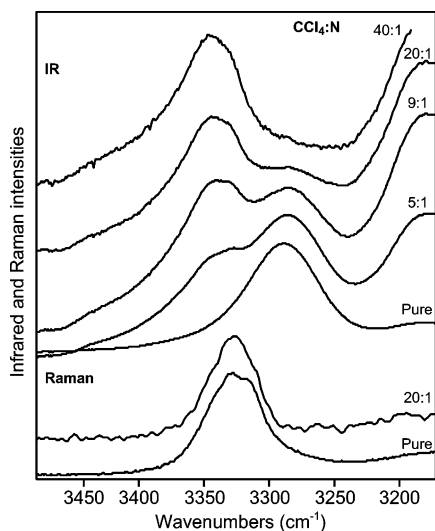


Figure 6. Infrared (top) and Raman (bottom) spectra of the N–H stretching region for pure DPA and DPA dissolved in carbon tetrachloride at different concentrations (reported as CCl_4/N molar ratios).

solution (not diluted), the presence of three $\nu_s(\text{SO}_3)$ bands at 1033, 1042, and 1051 cm^{-1} indicates that there are three different ionic species present. In the DMEDA–LiTf crystal, only one band occurs at 1063 cm^{-1} and is assigned to the $[\text{Li}_2\text{Tf}]^+$ species based on the crystal structure.³⁰ The similar frequencies (1033 and 1042 cm^{-1}) in the diluted samples and the nondiluted sample indicate that similar ionic species are present in the different samples. In the diluted samples, the ionic association seems to increase as more CCl_4 is added. However, the very complex interactions that occur in this system do not allow for a clear correlation between the triflate bands and the NH stretching bands. As in the HEXA system, it is probable that, upon dilution, the lithium–triflate interactions increase to the detriment of the lithium– NH_2 interactions.

3.3. Dipropylamine: A Simple Secondary Amine. The NH stretching vibrations of a simple secondary amine are also studied in CCl_4 . Figure 6 shows the IR and Raman spectra in the $\nu(\text{NH})$ region for pure DPA and DPA dissolved in CCl_4 at various molar ratios.

The IR spectrum of DPA consists of one broad band centered around 3289 cm^{-1} , whereas the Raman spectrum has two weak overlapping bands centered at 3327 and 3315 cm^{-1} . These data are consistent with the model used to explain the spectra of HEXA and DMEDA, where the IR spectrum samples molecules that are in a more hydrogen-bonded environment as reflected by a lower NH stretching frequency and the Raman spectrum samples molecules that are less hydrogen bonded. The presence of two different peaks in the Raman spectrum indicates two distinctly different types of weakly hydrogen-bonded NH groups in pure DPA.

As DPA is dissolved in CCl_4 , two broad bands around 3328 and 3346 cm^{-1} appear in the IR spectra. The growth of these bands with increasing dilution is accompanied by a decreasing intensity of the original 3289 cm^{-1} band. At a 9:1 CCl_4/NH molar ratio, the two new bands have about the same intensity, and at very high dilution, the band at 3346 cm^{-1} has the highest intensity, while the 3328 cm^{-1} band appears as a shoulder. The original band at 3289 cm^{-1} almost completely vanishes between the 20:1 and 40:1 compositions. In the Raman spectra, the frequency of the band at 3327 cm^{-1} does not shift when the concentration in DPA decreases, but its intensity rapidly

diminishes, as seen by the decrease in the signal-to-noise ratio. The second band at 3315 cm^{-1} slowly disappears upon dilution.

Wolff and Gamer studied hydrogen-bonding interactions in dimethylamine, a molecule very similar to DPA.^{31,32} In that work, when dimethylamine was dissolved in CCl_4 , two bands were observed in the IR spectra. One band around 3356 cm^{-1} increased with dilution and temperature and was attributed to free NH groups. The other band, whose intensity decreased with dilution and temperature, was attributed to hydrogen-bonded NH groups. They found two different populations of hydrogen-bonded groups: one at 3302 cm^{-1} when diluted in CCl_4 , and the other one at 3294 cm^{-1} in pure dimethylamine. Unfortunately, no Raman spectra were reported.

In the DPA– CCl_4 solution, the IR band at higher frequency (3346 cm^{-1}) probably originates in the “free” NH groups, i.e., the groups not involved in hydrogen bonding. The band at 3328 cm^{-1} appears to come from the vibrations of a hydrogen-bonded population of molecules that are diluted in CCl_4 . The intensity of the 3346 cm^{-1} band increases with CCl_4 dilution until, at the 40:1 dilution, it is the dominant feature in this region, with the 3328 cm^{-1} band appearing as a clearly discernible low frequency shoulder. The close overlap of these two broad features makes a spectral deconvolution very problematic. However, the qualitative trend in the relative intensities suggests a set of coupled equilibrium between species with different degrees of hydrogen bonding. It is clear that, with progressive dilution, the IR intensities of the “free” DPA band at 3346 cm^{-1} increases at the expense of the weakly hydrogen-bonded DPA band at 3328 cm^{-1} .

These results are similar to conclusions obtained from studies of hydrogen-bonding interactions in solvated alcohols, which have been the subject of numerous investigations.^{33–37} The general infrared characteristics of the OH stretching region are now well-known. In methanol, for example, the molecules form a highly hydrogen-bonded network. At various stages of dilution, many bands appear in the spectra and are assigned to the various species present: monomers (i.e., free molecules), dimers, and polymeric species. Analogously in DPA and its dilute solutions, the various bands may be assigned to different types of associated molecules such as dimeric and higher-order structures. These assignments are outside the scope of this paper.

The effect of adding salt to DPA is illustrated in Figure 7, which shows the IR spectra of DPA, DPA–LiTf 5:1, and DPA–LiTf 5:1 diluted in CCl_4 at various concentrations.

At all salt concentrations, the IR spectra have a band at 3302 cm^{-1} with a shoulder around 3346 cm^{-1} . As discussed previously, the band around 3346 cm^{-1} represents a population of DPA molecules undergoing limited or no hydrogen-bonding interactions and accordingly increases with dilution. As the solution becomes more concentrated in electrolyte, the band at 3302 cm^{-1} increases in intensity relative to the 3346 cm^{-1} band. This band is attributed to DPA molecules coordinated with the lithium cation.

In a previous study of the DPA–LiTf system, the crystal structure of DPA–LiTf, along with spectroscopic data of the crystal and DPA–LiTf solutions, were reported.²⁴ Upon addition of LiTf to DPA, no major shift in the band at 3289 cm^{-1} was observed, but the band became sharper until it split into two components at 3302 and 3288 cm^{-1} in the 5:1 composition (Figure 7); this splitting persisted in the crystalline state.²⁴ These two components were attributed to the two different environments for the hydrogen atom of the NH group that are found in the crystal structure: the latter band corresponds to the hydrogen atom that is weakly hydrogen bonded to a triflate oxygen, while

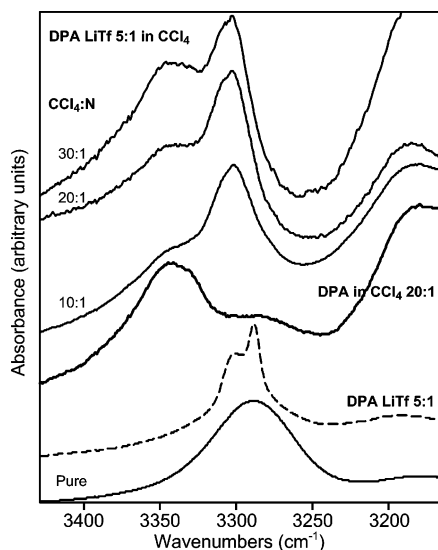


Figure 7. Infrared spectra of DPA–LiTf 5:1 (N/Li molar ratio) superposed with the infrared spectra of DPA diluted in CCl_4 at a 20:1 composition and DPA–LiTf 5:1 diluted in CCl_4 at different concentrations (reported as CCl_4/N molar ratios) in the N–H stretching region.

the other band corresponds to a “free” hydrogen atom. The correspondence between the band at 3302 cm^{-1} in the crystal and in the dilute CCl_4 solution shows that when DPA and LiTf in a 5:1 molar ratio are diluted in CCl_4 , the local NH_2 environment present in the crystal is preserved to some extent in the solution.

The triflate region strongly supports this argument. In the Raman spectra of the DPA–LiTf 5:1 dilute CCl_4 solutions, the $\nu_s(\text{SO}_3)$ band occurs at 1062 cm^{-1} and does not shift upon changing the electrolyte concentration. In the DPA–LiTf 5:1 sample (not diluted), the $\nu_s(\text{SO}_3)$ band also occurs at 1062 cm^{-1} . In the previous study, a careful comparison of the solution spectra with the crystal spectra determined that the nature of cation–anion interactions present in the solution phases (with N/Li ratio $\geq 5:1$) is very similar to that of the crystal, i.e., these interactions lead to the formation of the species $[\text{Li}_3\text{Tf}]^{2+}$. The NH stretching region of the spectra also showed strong similarities between the concentrated solution phases and the crystalline phase. It appears that, in the DPA–LiTf– CCl_4 system, the local environment of the amine group and the triflate ions is not affected by dilution in CCl_4 . When the electrolyte is dissolved in CCl_4 , there are local regions composed of the “undisturbed” electrolyte and local regions composed of DPA molecules that do not interact with lithium.

4. Conclusions

The dissolution of the different amines in carbon tetrachloride at high dilution has been shown to effectively eliminate intermolecular hydrogen-bonding interactions between the molecules. By comparing the Raman spectra (which selectively samples the least hydrogen-bonded molecules) with the infrared spectra (which are sensitive to the more hydrogen-bonded population), it was possible to recognize the different types of species present in solution. In HEXA dissolved in CCl_4 , two different types of molecules were identified from the NH stretching region: “free” molecules vibrating at high frequencies and hydrogen-bonded molecules vibrating at lower frequencies. In DMEDA, the same two populations were observed with N–H stretching frequencies very close to those of HEXA. Moreover, the presence of another type of interaction not present in HEXA was identified spectroscopically and attributed to DMEDA molecules forming intramolecular hydrogen bonds.

A number of authors have pointed out that, in the presence of strong intermolecular coupling, often arising from transition dipole interactions, the maximum of the infrared absorption of a particular normal mode does not necessarily occur at the same frequency as the maximum of the Raman scattering band from the same mode.^{38–40} This phenomenon has been termed the “noncoincidence effect”, although the same term has been applied to the case where the polarized Raman band maximum and the depolarized band maximum of a mode do not coincide due to strong intermolecular coupling. This effect may play a small role in the frequency shifts reported in this study. However, the changes in the hydrogen-bonding interactions are the dominant cause of the frequency shifts and intensity changes in the solutions studied here.

The overall picture of the hydrogen-bonding interactions developed in HEXA was shown to be applicable to the case of a simple secondary amine. In DPA, the spectrum might be expected to be relatively simple because there is only one N–H vibration for each amine group. However, the occurrence of two different bands in the Raman spectrum of pure DPA, as well as three different bands in the infrared spectra of the dilute DPA solutions in CCl_4 , suggested that there are two spectroscopically distinct classes of NH groups in weak hydrogen-bonded environments, as well as DPA molecules in a more strongly hydrogen-bonded environment.

When the amine–LiTf electrolytes were dissolved in carbon tetrachloride, the infrared and Raman spectra were extremely informative. In all of the systems studied, diluting the electrolytes in CCl_4 allowed for unambiguous identification of the shifts due to the cation coordination. In the Raman spectrum of HEXA–LiTf– CCl_4 , this effect was measured by a 22 cm^{-1} shift to lower frequencies. In the DMEDA–LiTf– CCl_4 solutions, the more complex hydrogen-bonding interactions complicated the analysis of the spectra, but the presence of three different populations was clear. Curve-fitting analysis of the spectra showed a direct correlation between two of the bands in the DMEDA and the HEXA systems corresponding to the “free” molecules and molecules affected by the lithium coordination. The band unique to the DMEDA system was again attributed to molecules that experience intramolecular hydrogen bonding.

The study of two different nitrogen/lithium molar ratios diluted to different concentrations in CCl_4 was extremely useful. As the N/Li⁺ ratio increased, the cation-shifted band increased in intensity accordingly, and as the solutions became more dilute in CCl_4 , the “free” band increased in intensity, allowing an unambiguous assignment of these features. The study of the symmetric SO_3 stretching mode brought little information in the DMEDA–LiTf– CCl_4 system. On the other hand, in HEXA comparisons between the symmetric SO_3 stretching mode and the NH stretching mode showed that, upon dilution, the lithium–triflate interaction increases while the lithium–amine interaction decreases. At high dilutions, where very limited N–H \cdots N hydrogen bonds remained, the lithium–triflate–amine interactions became more comparable (on a local basis) to those interactions in the crystalline phases. The spectra–structure correlation was particularly interesting in the DPA–LiTf system, where both the NH stretching and the SO_3 symmetric stretching regions indicated strong similarities between the crystalline phase and the solution phase in carbon tetrachloride.

Acknowledgment. N. M. Rocher thanks the Department of Chemistry and Biochemistry, University of Oklahoma, for financial support.

References and Notes

- (1) Wolff, H.; Schmidt, U. *Ber. Bunsen-Ges. Phys. Chem.* **1964**, *68*, 579.
- (2) Bellamy, L. J.; Williams, R. L. *Spectrochim. Acta* **1957**, *9*, 341.
- (3) Mason, S. F. *J. Chem. Soc. (London)* **1958**, 3619.
- (4) Sharpe, A. N.; Walker, S. *J. Chem. Soc. (London)* **1961**, 2974.
- (5) Stewart, J. E. *J. Chem. Phys.* **1959**, *30*, 1259.
- (6) Harris, C. S.; Ratner, M. A.; Shriver, D. F. *Macromolecules* **1987**, *20*, 1778.
- (7) Harris, C. S.; Shriver, D. F.; Ratner, M. A. *Macromolecules* **1986**, *19*, 987.
- (8) Paul, J.-L.; Jegat, C.; Lassegues, J.-C. *Electrochim. Acta* **1992**, *37*, 1623.
- (9) Tanaka, R.; Fujita, T.; Nishibayashi, H.; Saito, S. *Solid State Ionics* **1993**, *60*, 119.
- (10) Tanaka, R.; Ueoka, I.; Takaki, Y.; Kataoka, K.; Saito, S. *Macromolecules* **1983**, *16*, 849.
- (11) York, S.; Buckner, M.; Frech, R. *Macromolecules* **2004**, *37*, 994.
- (12) York, S.; Frech, R.; Snow, A.; Glatzhofer, D. *Electrochim. Acta* **2001**, *46*, 1533.
- (13) Rocher, N. M.; Frech, R. *Macromolecules* **2005**, *38*, 10661.
- (14) Frech, R.; York, S.; Allcock, H.; Kellam, C. *Macromolecules* **2004**, *37*, 8699.
- (15) Frech, R.; Huang, W. *Solid State Ionics* **1994**, *72*, 103.
- (16) Johnston, D. H.; Shriver, D. F. *Inorg. Chem.* **1993**, *32*, 1045.
- (17) Schantz, S.; Torell, L. M.; Stevens, J. R. *J. Chem. Phys.* **1991**, *94*, 6862.
- (18) Rhodes, C. P.; Frech, R. *Macromolecules* **2001**, *34*, 2660.
- (19) Rhodes, C. P.; Khan, M.; Frech, R. *J. Phys. Chem. B* **2002**, *106*, 10330.
- (20) Johansson, P.; Tegenfeldt, J.; Lindgren, J. *J. Phys. Chem. A* **1998**, *102*, 4660.
- (21) Frech, R.; Huang, W. *Macromolecules* **1995**, *28*, 1246.
- (22) Sutjianto, A.; Curtiss, L. A. *J. Phys. Chem. A* **1998**, *102*, 968.
- (23) Sanders, R. A.; Boesch, S. E.; Snow, A. G.; Hu, L. R.; Frech, R.; Wheeler, R. A.; Glatzhofer, D. T. *Polym. Prepr.* **2003**, *44*, 996.
- (24) Rocher, N. M.; Frech, R.; Khan, M. A. *J. Phys. Chem. B* **2005**, *109*, 20697.
- (25) Kakihana, M.; Schantz, S.; Torell, L. M. *J. Chem. Phys.* **1990**, *94*, 6271.
- (26) Schantz, S.; Sandahl, J.; Börjesson, L.; Torell, L. M.; Stevens, J. R. *Solid State Ionics* **1988**, *28–30*, 1047.
- (27) Huang, W.; Frech, R. *Polymer* **1994**, *35*, 235.
- (28) Huang, W.; Frech, R.; Wheeler, R. A. *J. Phys. Chem.* **1994**, *98*, 100.
- (29) Boesch, S.; Wheeler, R. Calculation of *N,N*-DMEDA, *N,N*-DMEDA–LiTf, and *N,N*-DMEDA–NaTf were performed using B3LYP, a hybrid Hartree–Fock density functional method, with a basis set of 6–31G(d), unreported results.
- (30) Rocher, N. M.; Frech, R.; Powell, D. *J. Phys. Chem. B* **2006**, *110*, 15117.
- (31) Wolff, H.; Gamer, G. *J. Phys. Chem.* **1972**, *76*, 871.
- (32) Buttler, M. J.; McKean, D. C. *Spectrochim. Acta* **1965**, *21*, 465.
- (33) Kristiansson, O. *J. Mol. Struct.* **1999**, *477*, 105.
- (34) Liddel, U.; Becker, E. D. *Spectrochim. Acta* **1957**, *10*, 70.
- (35) Symons, M. C. R.; Thomas, V. K. *J. Chem. Soc., Faraday Trans. I* **1981**, *77*, 1883.
- (36) Jeffrey, G. A. *An Introduction to Hydrogen Bonding*; Oxford University Press: New York, 1997.
- (37) Pimental, G. C.; McClellan, A. L. *The Hydrogen Bond*; W. H. Freeman: San Francisco, 1960.
- (38) Torii, H.; Musso, M.; Giorgini, M. G. *J. Phys. Chem. A* **2005**, *109*, 7797.
- (39) Bertie, J. E.; Michaelian, K. H. *J. Chem. Phys.* **1998**, *109*, 6764.
- (40) Mortensen, A.; Nielsen, O. F.; Yarwood, J.; Shelly, V. *J. Phys. Chem.* **1994**, *98*, 5221.